Am J Cancer Res 2016;6(9):1906-1921
www.ajcr.us /ISSN:2156-6976/ajcr0035784

Original Article

iPSC-derived cancer stem cells provide a model of tumor vasculature

Marta Prieto-Vila[1], Ting Yan[2], Anna Sanchez Calle[1], Neha Nair[1], Laura Hurley[3], Tomonari Kasai[1], Hiroki Kakuta[4], Junko Masuda[1], Hiroshi Murakami[1], Akifumi Mizutani[1], Masaharu Seno[1]

[1]Department of Biotechnology, Graduate School of Natural Science and Technology, Okayama University, 3.1.1 Tsushima-Naka, Kita-ku, Okayama 700-8530, Japan; [2]Translational Medicine Research Center, Key Laboratory of Cellular Physiology, Ministry of Education, Shanxi Medical University, 56# Xinjian South Road, Taiyuan 030001, Shanxi, China; [3]Cancer Biology Graduate Program, School of Medicine, Wayne State University, 10 E Warren Avenue, Suite 2215, Detroit, Michigan 48201, USA; [4]Laboratory of Bioorganic and Medicinal Chemistry, Graduate School of Medicine, Dentistry and Pharmaceutical Sciences, Okayama University, 1-1-1 Tsushima-Naka, Kita-ku, Okayama 700-8530, Japan

Received July 14, 2016; Accepted July 18, 2016; Epub September 1, 2016; Published September 15, 2016

Abstract: To grow beyond a size of approximately 1-2 mm^3, tumor cells activate many processes to develop blood vasculature. Growing evidences indicate that the formation of the tumor vascular network is very complex, and is not restricted to angiogenesis. Cancer cell-derived tumor vasculatures have been recently described. Among them, endothelial differentiation of tumor cells have been directly related to cancer stem cells, which are cells within a tumor that possess the capacity to self-renew, and to exhibit multipotential heterogeneous lineages of cancer cells. Vasculogenic mimicry has been described to be formed by cancer cells expressing stemness markers. Thus, cancer stem cells have been proposed to contribute to vasculogenic mimicry, though its relation is yet to be clarified. Here, we analyzed the tumor vasculature by using a model of mouse cancer stem cells, miPS-LLCcm cells, which we have previously established from mouse induced pluripotent stem cells and we introduced the DsRed gene in miPS-LLCcm to trace them *in vivo*. Various features of vasculature were evaluated *in ovo*, *in vitro*, and *in vivo*. The tumors formed in allograft nude mice exhibited angiogenesis in chick chorioallantoic membrane assay. In those tumors, along with penetrated host endothelial vessels, we detected endothelial differentiation from cancer stem cells and formation of vasculogenic mimicry. The angiogenic factors such as VEGF-A and FGF2 were expressed predominantly in the cancer stem cells subpopulation of miPS-LLCcm cells. Our results suggested that cancer stem cells play key roles in not only the recruitment of host endothelial vessels into tumor, but also in maturation of endothelial linage of cancer stem cell's progenies. Furthermore, the undifferentiated subpopulation of the miPS-LLCcm participates directly in the vasculogenic mimicry formation. Collectively, we show that miPS-LLCcm cells have advantages to further study tumor vasculature and to develop novel targeting strategies in the future.

Keywords: Cancer stem cells, tumor vasculature, vasculogenic mimicry, differentiation, angiogenesis, endothelial cell, CAM assay, tube formation

Introduction

Tumors can only grow to a size of approximately 1-2 mm^3 before reaching their metabolic demand [1]. To grow beyond this size, tumor cells undergo the process known as angiogenesis [1]. Angiogenesis, firstly described by Folkman in 1971 [2], is a progressive, multistep physiological process by which new blood vessels are developed from preexisting vessels [3]. These vessels are in charge of the supply of nutrients and oxygen to sustain tumor tissues.

Tumor angiogenesis starts with the activation of endothelial cells (EC) by inflammatory cytokines and angiogenic factors released by tumor cells, such as vascular endothelial growth factor (VEGF), fibroblast growth factor (FGF) and platelet derived growth factor (PDGF), which stimulate a cascade of endothelial changes and promote them to secrete several proteases and plasminogen activators, resulting in the degradation of the vessel basement membrane, allowing EC to invade the surrounding membrane [4, 5]. Then, cells proliferate and eventu-

ally migrate to form new vessels. Finally, the endothelial cells deposit a new basement membrane and secret growth factors that attract support cells such as pericytes, ensuring the stability of the new vessels [6]. With targeting EC specific molecules, many therapeutic strategies have been developed to interfere with the formation of tumor blood vessels. For example, bevacizumab, an antibody against VEGF receptors, has been tested in many types of solid tumor [6, 7]. Unfortunately, despite the efforts, most of these treatments failed to reveal the expected results [8].

Accumulating knowledge regarding the complexity of tumor vasculogenesis might explain, at least in part, the failure of the classical anti-angiogenic drugs targeting ECs. Vasculogenic mimicry (VM), a concept which was first described in 1999 by Maniotis et al., is a process for tumor vasculature generation found in malignant and poorly differentiated tumors, in which tumor cells themselves generate organized networks of vessels. The VMs channels are rich in extracellular matrix (ECM), but are typically without CD31 positive endothelial cells [9, 10]; therefore, VM should not rely on typical essential angiogenic markers [11]. EphA2-VE cadherin connection, Tie1, Slpi and Serpine2 have been described as important factors for the structure of VM [12-15]. VM has been found in many kinds of tumors such as glioblastoma [9, 16], hepatoma [11], melanoma [10] and colon cancer [17].

Another concern related to tumor vasculogenesis is the contribution of cancer stem cells (CSCs). CSCs are cells within a tumor that possess the capacity to self-renew and to exhibit multipotential heterogeneous lineages of cancer cells that comprise the tumor [18], and are thought to be responsible for various cancer pathologies, such as metastasis or recurrence due to CSC's exhibiting higher drug resistance compared to other tumor cells. CSCs have also been thought to be responsible for tumor vasculogenesis. One of the most significant findings regarding tumor vasculogenesis is the direct differentiation of glioblastoma $CD133^+$ CSCs into vascular endothelial cells expressing CD31 when these cells were injected into nude mice [19, 20]. Additionally, breast and renal CSCs differentiated after 14 days of incubation under hypoxia and with VEGF containing complete medium *in vitro* [21].

In addition to the direct differentiation into endothelial cells, the high degree of plasticity of CSCs and the fact that cells lining the channels express stemness-related genes [1, 22] indicate that CSCs might be involved in VM. Currently there is no clear evidence that demonstrates the direct relation of CSCs and VM.

The processes of tumor vasculogenesis should therefore be investigated with the consideration of the properties of CSCs. To understand the entire process of tumor vasculogenesis, the development of a model of CSCs and tumor should be helpful. Our laboratory has generated models of CSC (miPS-CSCs) that were spontaneously converted from mouse induced pluripotent stem cells (miPS) cultured in the presence of conditioned medium (CM) from various cancer cell lines. We reported previously that miPS-LLCcm, a representative miPS-CSC converted with CM of Lewis lung carcinoma (LLC) cells, formed highly angiogenic tumors in nude mice, and exhibited the capacity of differentiation into endothelial cells *in vitro* [23]. However, the origin of the cells in the vascular structures in the tumor formed by miPS-LLCcm has not been assessed directly. In this study, we evaluated angiogenesis, CSC's differentiation into ECs, and VM, along with their possible correlations during the vasculature development in the tumors of miPS-LLCcm cells.

Materials and methodology

Construction of DsRed expression vector

The DsRed2 gene was amplified from pCI-EGFP/DsRed2-puro by PCR with a primer pair; *Eco*RI-DsRed (5'-CCGGAATTCATGGCCTCTCC-3') and *Sal*I-DsRed (5'-TCCGGTCGACCTACAGGAACAG-3') to add *Eco*RI and *Sal*I sites to the 5' and 3' end of Ds-Red gene, respectively. Then, the PCR product was cloned downstream of EF-1 alpha constitutive promoter in pEF-EX-HA vector, which was constructed by adding an HA tag to pEF-BOS-EX [24] with the similar construction procedure of Flag tag described in [25], to create pEF-DsRed. For pEF-neo plasmid construction, the G418 resistant gene was amplified from pST-Neo by PCR with a primer pair *Eco*RI-neo (5'-GCCGGAATTCATGATTGAACAAGATGGA-3') and *Sal*I-neo (5'-TGTAGTCGACTCAGAAGAACTCGTCAAG-3') to add *Eco*RI and *Sal*I sites to the 5' and 3' sites of the gene. Amplified gene was cloned into pEF-EX-HA.

Cell culture and transfection

Mouse LLC cells were purchased from ATCC (Manassas, VA) and were maintained in Dulbecco's Modified Eagle's Medium-high glucose (DMEM, Sigma, MO) containing 10% FBS (Gibco, NY) and 100 U/mL penicillin/streptomycin (Wako, Japan). miPS were cultured in DMEM containing 15% FBS, 0.1 mM MEM Non-Essential amino acids, (100X NEAA, Gibco, NY), 2 mM L-Glutamine (Nacalai Tesque, Japan), 0.1 mM 2-mercaptoethanol, 50 U/ml penicillin/streptomycin and 1000 U/mL Leukemia inhibitory factor (LIF, Millipore, MA). miPS-LLCcm cells were cultured in miPS media without LIF. All the cells were maintained at 37°C in the atmosphere of 5% CO_2. Medium was changed every two days.

For transfection, 1×10^7 miPS-LLCcm cells, which were maintained in suspension culture for 8 days, in 600 µL electroporation buffer for ES cells (Millipore, MA) were mixed with 1 µg of linearized pEF-neo DNA and 10 µg of linearized pEF-DsRed DNA. Then, the cell suspension was transferred into a 0.4 cm gap-cuvette and electroporated by using Gene Pulser II (Bio Rad Labs, VA). The cells were then plated into gelatin-coated dishes without antibiotics for 2 days. Then the DsRed positive transfectants (termed DsRed-LLCcm) were established by culturing for 1 to 2 weeks in the presence of G418 at a concentration of 0.3 mg/mL.

For selection of GFP-positive undifferentiated cells of miPS-LLCcm and DsRed-LLCcm, cells were cultured in the miPS medium containing 1 mg/mL puromycin for 7 days, changing the medium daily [27, 28].

Sphere formation assay

4×10^4 cells (1×10^4 cells/ml) were seeded on 6 cm ultra low attachment dishes (Corning incorporated, NY) with the miPS media without FBS, but supplied with Insulin-Transferrin-Selenium-X (ITS-X, Life Technologies, CA). Cells were cultured at 37°C under 5% CO_2 for 4 days, and the spheroids with diameters above 100 µm were judged as self-renewing spheroids.

In vitro tube formation assay

5×10^4 cells were seeded on growth factors reduced Matrigel (Corning, NY) -coated 96 well plate and cultured in 50 microL of EBM2 media (EBM-2 Single Quots Kit, Lonza, Switzerland) for 24 hr in the presence or absence of angiogenic factors (FBS, hydrocortisone, hFGF-B, VEGF, R3-IGF-1, hEGF, ascorbic acid, GA-1000 and heparin). The experiments were performed in triplicate. Images of formed tubes were captured by Olympus CKX41 microscope, or Keyence BZ-X700.

Animal experiments

Nude mice (Balb/c-nu/nu, female, 4 weeks old) were purchased from Charlesriver, Japan. For transplantation studies, 1×10^6 cells were suspended in 200 µL in the miPS-media and injected subcutaneously in both flanks of mice (n=4). Tumor volumes were measured every 3-4 days and calculated as following formula (0.5× longer diameter × shorter diameter^2). After 5 weeks, tumors were extracted and separated in 4 equal parts that were used for the primary cell culture, histological analysis, immunofluorescent analysis, and CAM assay experiment as described below.

The plan of animal experiments was reviewed and approved by the ethics committee for animal experiments of Okayama University under the ID OKU-2013252, OKU-2016078.

Chick embryo chorioallantoic membrane (CAM) assay

Fertilized eggs were obtained from Yamagishi (Mie, Japan), and sterilized with ethanol 70% to *a posteriori* incubated at 37°C in 60% of humidity in a incubator P-008(B) (Showa Furani, Japan). After acclimatization for 2 days, 3 mL of egg white was extracted using an 18G hypodermic needle and 5 mL syringe generating an air sac directly over the chick embryo chorioallantoic membrane (CAM). On the day 8, an approximately 1 cm^2 window was opened in the shell of an egg and the 5 mm^3 portions of the tumor extracted from the grafted mice was collocated over the CAM with sterilized plastic ring. For the control, only the plastic ring was located on CAM. The window was sealed with transparent tape, then, the eggs were incubated. Images of vasculature were taken on day 12 after injecting 2 mL of 20% Intralipos (Otsuka Pharmaceutical, Japan) under the membrane.

Histological analysis and immunohistochemistry

Extracted tumors were enveloped with paraffin and sectioned at 5 µm of thickness. After depa-

raffinization, sections were stained with hematoxylin-eosin (Hemaoxylin solution, Sigma-Aldrich, MO; 0.5% Eosin Y, Sigma Aldrich, MO) and Periodic Acid-Schiff (PAS, Millipore, MA) for histological analysis. For immunohistochemistry of GFP, DsRed, Ki67 and CD31, antigen retrieval was carried out by boiling in 10 mM citrate sodium (pH6) with 0.05% Tween20 for 15 min. After cooling down the samples, the endogenous peroxidase was blocked with 3% H_2O_2 for 5 min. Ellite anti-rabbit ABC staining Vectastain kit (Vector, MI) and 3,30-diaminobenzidine tetrahydrochloride (DAB, Vector, MI) were used for detection of GFP, Ki67 and DsRed with rabbit monoclonal anti-GFP antibody (1:400, #2956, Cell Signaling, MA) Ki67 (1:200, #ab66155, Abcam, UK) and rabbit polyclonal anti-DsRed (1:100, #ab62341, Abcam, UK), respectively. Counter staining was carried out using hematoxylin.

For CD31-PAS double staining, Ellite anti-rabbit ABC Vectastain kit was also used. Rabbit polyclonal anti CD31 (1:100, #ab28364, Abcam) was incubated for 2 hr at room temperature, and immunoreactivity was also detected by using DAB. Afterwards, tissues were stained with PAS solution by following manufactures protocol, omitting hematoxylin counterstaining to reduce visual noise. These sections were viewed under light microscopy (FSX100, Olympus, Japan).

Immunofluorescence analysis

The freshly extracted tumor tissue samples were embedded with Tissue-Tek OCT compounds (Sakura Finetek, CA), frozen and sectioned into the 10 μm thickness. Cryosections were fixed with Paraformaldehyde phosphate buffer solution 4% (PFA, Nacalai Tesque, Japan) for 20 min at room temperature, followed by permeabilization with 0.05% Tween20 in PBS (PBS-T). After blocking with PBS-T containing 5% BSA, cryosections were incubated with primary antibodies (rat monoclonal anti-PECAM1 (1:50, sc-101454, Santa Cruz) and rabbit polyclonal anti-DsRed (1:100, ab62341, Abcam) for overnight at 4°C. Following washes with PBS-T, sections were incubated with secondary antibodies Texas Red-X conjugated goat anti-rat IgG (1:500, #6392, Invitrogen, CA) and Alexa Fluor 488 donkey anti rabbit IgG (1:500, #A21206, Life Technologies, CA). Nuclei were counterstained with 4',6-diamidino-3-phenylidole, dihydrochloride (DAPI, Vector, MI).

For staining of *in vitro* formed tubes, 1.5×10^6 cells were seeded on 8-well chamber slides (Corning, NY) and for the staining of in vitro culture, cells were seeded on gelatin-coated cover glasses. After incubation, cells were fixed, permeabilized, and stained with rabbit polyclonal anti-CD31 antibody (1:100, #ab28364, Abcam, UK) and Alexa Fluor 555 conjugated anti-rabbit IgG (1:500, #A21428, Life technologies, CA).

Images were acquired using an Olympus IX81 microscope equipped with a light fluorescence device (Olympus, Japan).

RNA extraction, cDNA synthesis and quantitative real time PCR

Total RNA from cells was isolated using RNeasy Mini Kit (QIAGEN, Germany), then treated with DNase I (Takara, Japan). 1 μg of RNA was reverse transcribed using SuperScript III First strand kit (Invitrogen, CA).

Quantitative real-time PCR was performed with Cycler 480 SYBR Green I Master mix (Roche, Switzerland) according to manufacturer's instructions. Primers used for the real time qPCR were as following (forward and reverse). Sox2 5'-TAGAGCTAGACTCCGGGCGATGA-3' and 5'-TTGCCTTAAACAAGACCACGAAA-3'; Oct3/4 5'-TCTTTCCACCAGGCCCCCGGCTC-3' and 5'-TGCGGGCGGACATGGGGAGATCC-3'; Klf4 5'-GCGAACTCACACAGGCGAGAAACC-3' and 5'-TCGCTTCCTCTTCCTCCGACACA-3'; c-Myc 5'-TGACCTAACTCGAGGAGGAGCTGGAATC-3' and 5'-AAGTTTGAGGCAGTTAAAATTATGGCTGAAGC-3'; VEGF-A 5'-ATGAACTTTCTGCTCTCTTGGGTGC-3' and 5'-CATGGGACTTCTGCTCTCCTTCTG-3'; FGF2 5'-CCTTCCCACCAGGCCACTTCAA-3' and 5'-GGTCCCGTTTTGGATCCGAGTTT-3'. Gene expression level was normalized with that of GAPDH mRNA.

Statistical analysis

All quantitative data is expressed as mean ± SD and statistically analyzed by Student's t-test. A *p*-value lower than 0.05 was considered as statistically significant.

Results

Establishment of DS Red-expressing miPS-LLCcm, DsRed-LLCcm

We have previously established models of CSCs, named miPS-CSCs, that were derived from miPSCs by culturing them with condi-

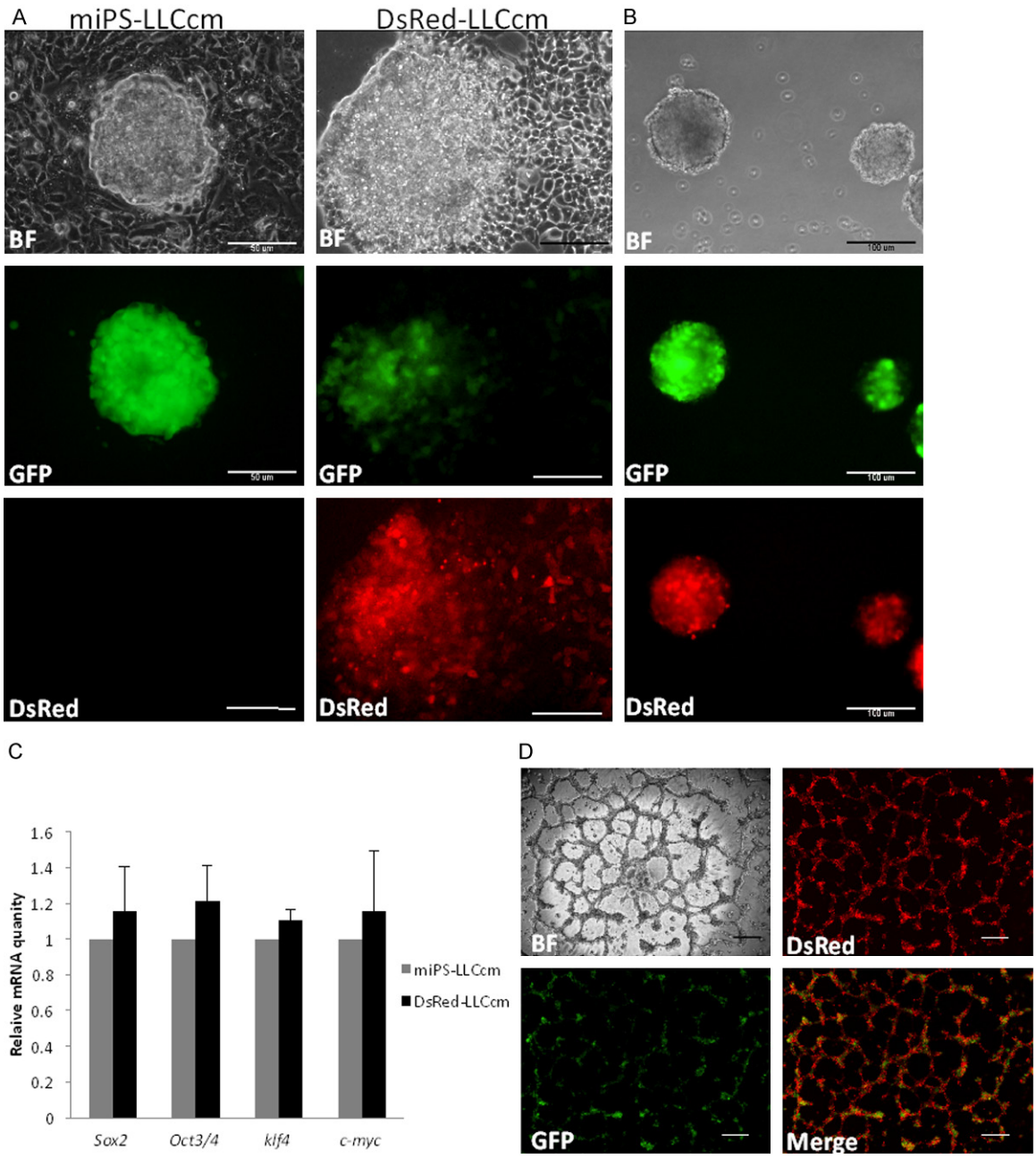

Figure 1. Establishment of Ds-Red expressing miPS-LLCcm, DsRed-LLCcm. A: Morphology of miPS-LLCcm and DsRed-LLCcm cells. Under the control of EF1 promoter, DsRed was expressed constitutively. Scale bar: 50 μm. B: Sphere formation of DsRed-LLCcm cells, all the spheres are GFP$^+$ and DsRed$^+$. Scale bar: 100 μm. C: Expression levels of Sox2, Oct3/4, Klf4, and C-myc in DsRed-LLCcm cells were analyzed by RT-qPCR. Equivalent expressions of those genes in comparison to miPS-LLCcm were confirmed (Sox2 P=0.71; Oct3/4 P=0.45; Klf4=0.20; c-myc P=0.73). Expression values are normalized to GAPDH. D: In vitro tube formation of DsRed-LLCcm cells. Scale bar: 200 μm.

tioned medium prepared from various cancer cells or cancer cell derived microvesicles/exosomes [23, 26]. We have proposed that these models are very promising to study cancer's nature from the aspect of CSCs properties, such as the relation between CSCs and differentiated cancer cells [23, 27]. miPS-LLCcm cells, a representative model of CSCs converted from miPSCs with the conditioned medium of LLC cells, generated malignant, highly vascularized tumors when they were transplanted in nude mice. In addition, we could reveal the dif-

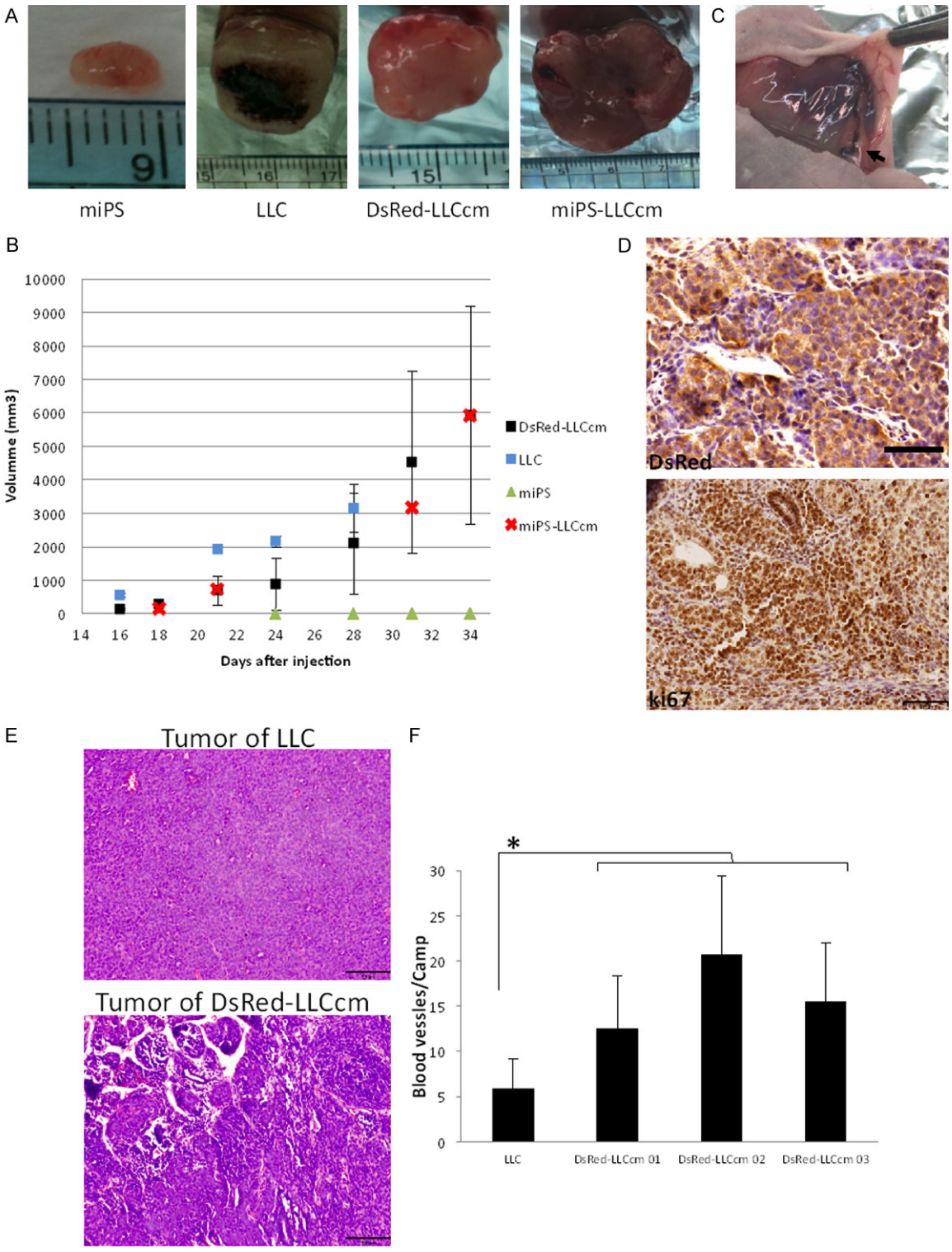

Figure 2. DsRed-LLCcm cells form malignant and highly angiogenic tumor *in vivo*. A: Images of tumors formed by indicated cells. B: Growth rate of tumors. LLC (n=2), DsRed (n=4), miPS (n=3), miPS-LLCcm (n=1). C: A typical image of blood vessels surrounding the tumor of DsRed-LLCcm. D: Immunohistochemistry of DsRed (upper panel) and Ki67 (lower panel) of tumor derived from DsRed-LLCcm cells. Scale bar: 50 μm. E: Hematoxylin-Eosin staining images of LLC and DsRed-LLCcm derived tumor. Scale bar: 100 μm. F: Blood vessel density of LLC and DsRed-LLCcm derived tumor. Random camps (n=15) were pictured and all the channels that contained red blood vessels were counted. *P<0.05.

ferentiation capacity of miPS-LLCcm cells into endothelial cells *in vitro* [26, 27]. In the previous study, however, it remained unclear whether the cells forming the vasculature in the tumor are derived from miPS-LLCcm or not. To confirm whether the cells forming the vasculature in the tumor originated from miPS-LLCcm cells or host mouse cells, we established DsRed-LLCcm cells introducing pEF-DsRed into miPS-LLCcm cells. Since miPS-LLCcm cells were derived from Nanog-GFP-iPSCs [28], the undifferentiated state could be monitored by the expression of GFP together with that of DsRed. On the other hand, the cells differentiated from miPS-LLCcm cells would display only DsRed fluorescence (**Figure 1A**).

First, we evaluated whether DsRed-LLCcm retained miPS-LLCcm properties. Self-renewal was assessed by sphere formation assay [29]. DsRed-LLCcm cells were able to form spheres under non-adherent conditions as miPS-LLCcm did (**Figure 1B**). All the spheres derived from DsRed-LLCcm were GFP and DsRed positive. Supporting their stemness state, the expression levels of endogenous Oct3/4, Sox2, Klf4 and c-Myc were comparable to those in miPS-LLCcm cells (**Figure 1C**). DsRed-LLCcm cells were also able to generate tube-like structures when the cells were seeded on Matrigel (**Figure 1D**), as miPS-LLCcm cells did [23, 27]. Similar to miPS-LLCcm cells, this tube formation was not dependent on the supplement of endothelial cell growth factor such as VEGF or FGF (data not shown). The entire tubular structures possessed fluorescence of DsRed. In contrast, GFP positive cells were found to be concentrated on the nodules of the tubes, where two or more tubular structures are connected (**Figure 1D**).

Along with *in vitro* characterization, we evaluated the tumorigenicity of DsRed-LLCcm cells by transplanting 10^6 DsRed-LLCcm cells subcutaneously into nude mice. miPS-LLCcm cells, miPS cells, and LLC cells were also transplanted for comparison (**Figure 2A**). We observed that all tumors, except for miPS cells, started to grow rapidly after two weeks of transplantation. The growth rates of DsRed-LLCcm tumors were similar to those of miPS-LLCcm tumors (**Figure 2B**). The tumor derived from LLC cells had the highest growth rate. However, the tumor showed significant necrotic features on the third week (**Figure 2A**). On the other hand, tumors derived by DsRed-LLCcm and miPS-LLCcm cells kept growing without any apparent signatures of necrosis, and host vessels were found to be directed towards the tumor (**Figure 2C**). Immunohistochemical analysis of DsRed-LLCcm tumors showed that most of the cells forming the tumor expressed DsRed (**Figure 2D**, up), and the staining with Ki67 antibody revealed that the cells in the DsRed-LLCcm tumors were highly proliferative (**Figure 2D**, down), supporting the rapid tumor growth. Next, LLC tumor and the three replicates of DsRed-LLCcm tumor were histologically compared, and the density of blood vessels was counted (**Figure 2E**, **2F**). While the LLC tumor showed relatively homogenous structure and fewer blood vessels, DsRed-LLCcm tumors constructed unorganized, heterogeneous structures with higher amount of blood vessels (**Figure 2E**). The vessel structures containing blood cells in the tumor of DsRed-LLCcm were significantly abundant when compared to those found in the tumor of LLC cells (**Figure 2F**). These could help to explain the observation of necrosis in the LLC derived tumor, but not in the DsRed-LLCcm derived tumor which continuously grew without visible necrosis.

These features of the DsRed-LLCcm tumor were indistinguishable from the tumor formed by miPS-LLCcm [23]. Taken together *in vitro* and *in vivo* properties, we concluded that the introduction of DsRed2 gene did not affect the CSC properties in miPS-LLCcm cells. Thus, we used DsRed-LLCcm cells for tracing differentiated cells *in vivo*.

Recruitment of blood vessels from the host by DsRed-LLCcm cells

Tumor angiogenesis is described as the process by which new blood vessels are developed from preexisting vessels [3]. Since we had observed host blood vessels surrounding the tumors derived from miPS-LLCcm and DsRed-LLCcm (**Figure 2C**) and high amount of vessels within those tumors (**Figure 2E**, **2F**), we further confirmed the recruitment of preexisting blood vessels to the tumors by using CAM assay [30]. In this study, we implanted a tumor portion of 5-mm-cube on CAM which was freshly extracted from grafted mouse (**Figure 3A**). Both tumors of DsRed-LLCcm and LLC promoted chick blood vessels formation when compared with the negative control (**Figure 3B**, **3C**). In

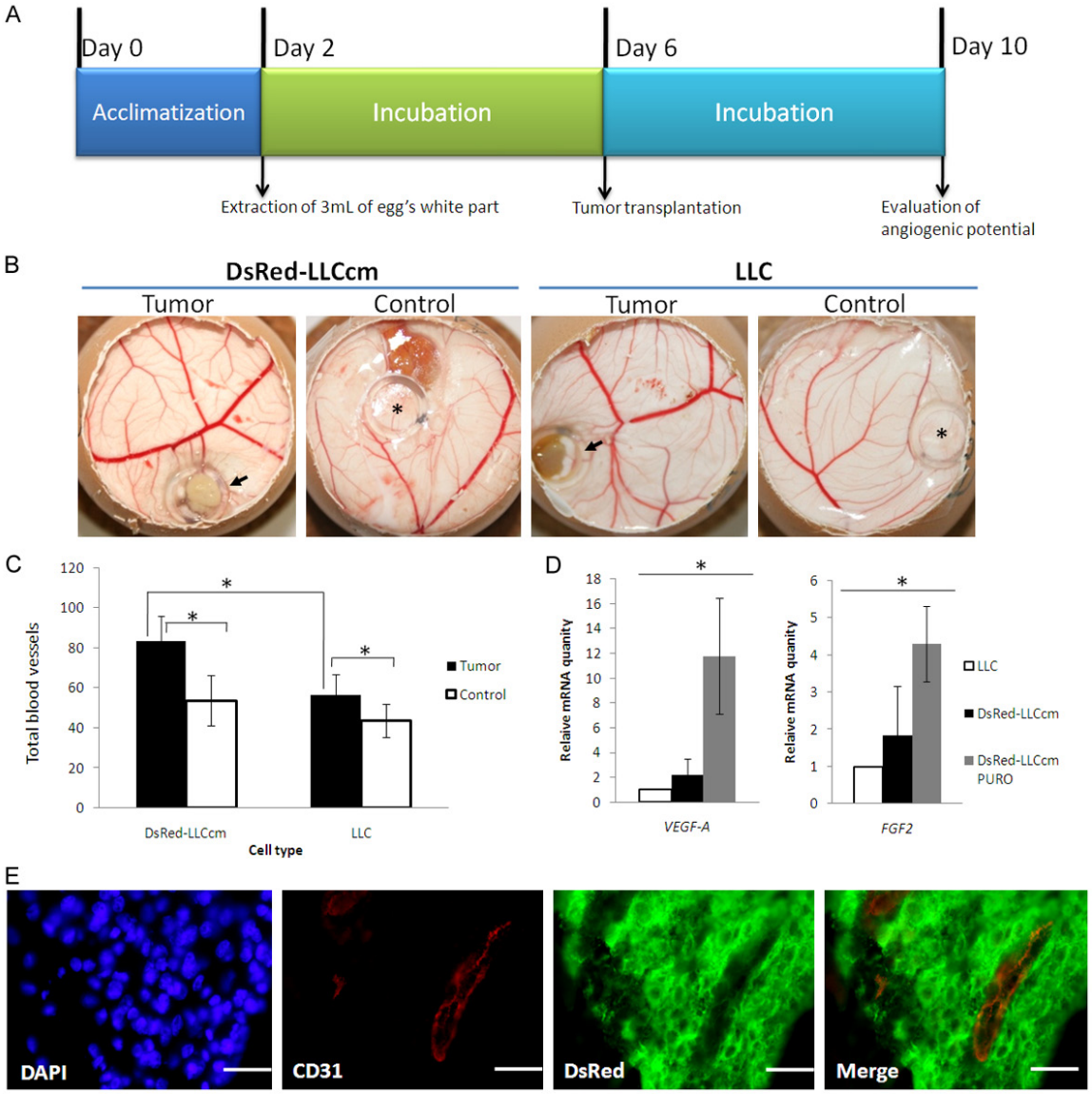

Figure 3. Angiogenic properties of DsRed-LLCcm cells. A: Experimental scheme of CAM assay. On day 6, a piece of freshly isolated tumor was added on the CAM, and on day 10, the pictures were taken and results analyzed. B: Typical results of CAM assay. C: Quantitative evaluation of blood vessel number in CAM assay. *P<0.05. D: Expression of VEGF-A and FGF2 in DsRed-LLCcm and DsRed-LLCcm selected with puromycin in comparison to LLC cells were quantified by RT-qPCR. Expression values are normalized to GAPDH. *P<0.05. E: Immunofluorescence analysis using CD31 (red)- and DsRed (green)-antibodies in tumors derived from DsRed-LLCcm cells. Scale bar: 25 μm.

addition, a significantly higher number of blood vessels towards the tumor of DsRed-LLCcm cells than of LLC cell-derived tumor was observed (8.8±3.3 and 5.6±1.9, respectively), indicating a higher ability of recruitment of blood vessels in DsRed-LLCcm tumor. To support this, the expression of VEGF-A in DsRed-LLCcm cells was found to be higher than that in LLC cells (**Figure 3D**, left). Interestingly, the expression level of VEGF-A was dramatically higher when the undifferentiated subpopulation of sRed-LLCcm cells was concentrated by culturing with puromycin. This result suggested that VEGF-A could be secreted from CSCs predominantly. This was also observed in FGF2 expression (**Figure 3D**, right). The expression of angiogenic factors in CSCs could explain the results of the *in vitro* tube formation assay that were independent of exogenous angiogenic factors [27].

Furthermore, we could confirm the existence of penetrated host blood vessels in the tumor generated by DsRed-LLCcm. On week 5 of

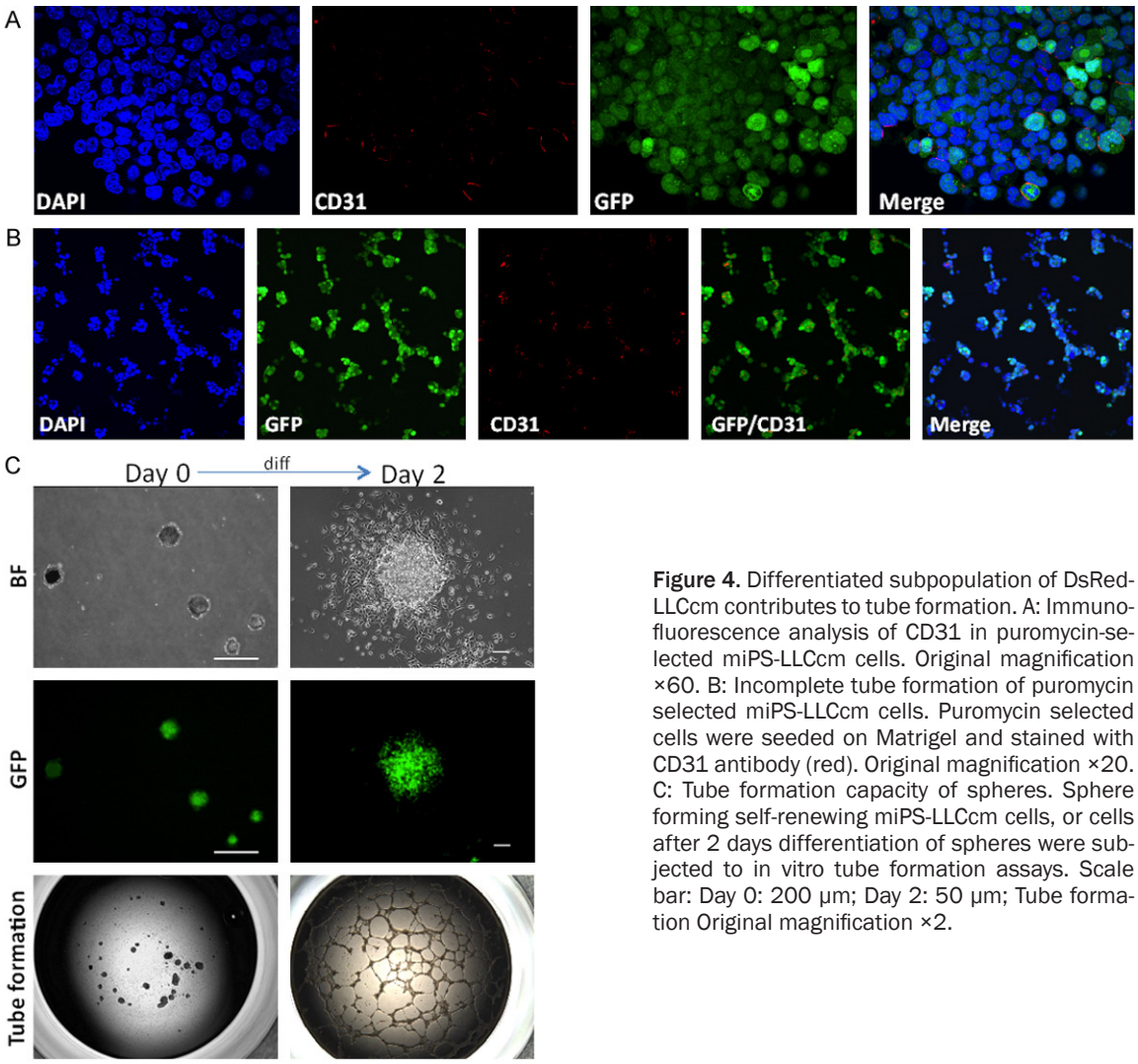

Figure 4. Differentiated subpopulation of DsRed-LLCcm contributes to tube formation. A: Immunofluorescence analysis of CD31 in puromycin-selected miPS-LLCcm cells. Original magnification ×60. B: Incomplete tube formation of puromycin selected miPS-LLCcm cells. Puromycin selected cells were seeded on Matrigel and stained with CD31 antibody (red). Original magnification ×20. C: Tube formation capacity of spheres. Sphere forming self-renewing miPS-LLCcm cells, or cells after 2 days differentiation of spheres were subjected to in vitro tube formation assays. Scale bar: Day 0: 200 μm; Day 2: 50 μm; Tube formation Original magnification ×2.

tumor growth, the tumor was stained with anti-CD31 antibody and anti-DsRed antibody. $CD31^+/DsRed^-$ cells with channel-like structure were found frequently, showing that these blood vessels were originated from host animal (**Figure 3E**). Thus, our results suggest that CSCs should contribute to angiogenesis directly by secreting angiogenic factors.

Existence of endothelial cells differentiated from CSCs in vitro and in vivo

As reported in previous studies, miPS-LLCcm cells were able to differentiate into endothelial cells, and were able to form tube-like structures composed by $CD31^+/GFP^-$ differentiated cells, $CD31^-/GFP^+$ undifferentiated cells and $CD31^+/GFP^+$ bipotential cells on Matrigel [26, 27]. The formation of the tubular structure required differentiated population, since neither GFP^+ (both $CD31^-/GFP^+$ and $CD31^+/GFP^+$) cells concentrated by puromycinin adherent culture (**Figure 4A**) nor GFP^+ self-renewing spheres were able to form the structure directly (**Figure 4B**) [27]. In contrast, when spheres were seeded into adherent culture for two days to give rise to GFP^- differentiated cells; these cells were able to generate tube structures (**Figure 4C**).

The bulk culture of miPS-LLCcm cells consists of 2 distinct kinds of morphologies: cells forming GFP^+ embryonic stem (ES)-like colonies and GFP^- differentiated cells (**Figure 1A**) [23]. We stained the bulk culture of miPS-LLCcm cells with anti-CD31 antibody, and found that $CD31^+$ cells were detected (**Figure 5A**, **5B**). As found in the tube formation, $CD31^+/GFP^-$ differentiated cells, $CD31^-/GFP^+$ undifferentiated cells, and

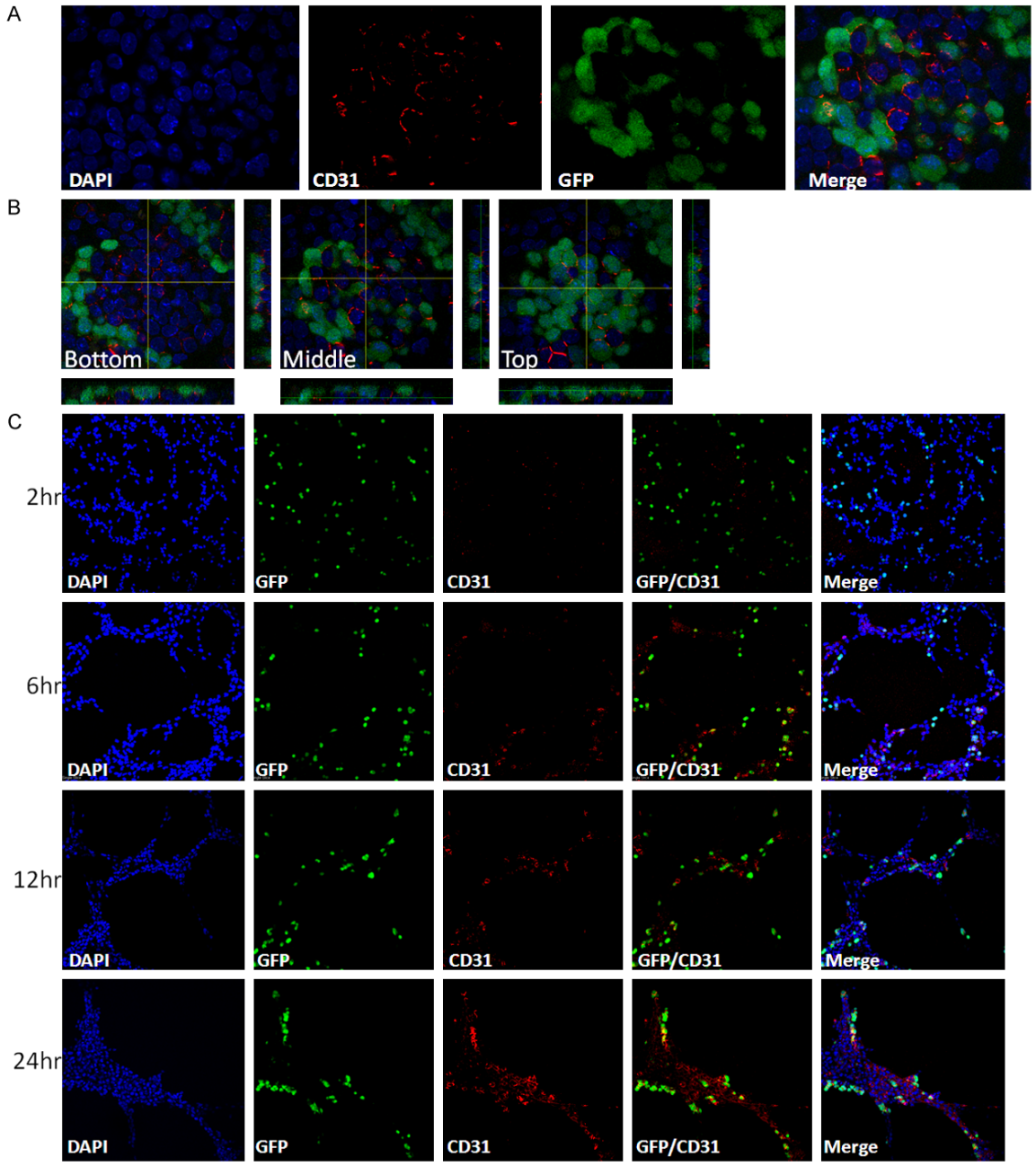

Figure 5. Differentiation and maturation of endothelial cells from miPS-LLCcm. (A) Immunofluorescence analysis of CD31 (red) in bulk culture of miPS-LLCcm cells, original magnification ×100. (B) 3D image of (A). The images show three different height sections of the same ES-like colonies of cells, original magnification ×100. (C) Time course analysis of in vitro tube formation. Cells were stained with CD31 (red) antibody at indicated time, original magnification ×20.

$CD31^+/GFP^+$ bipotential cells were present in the bulk culture. Interestingly, $CD31^+$ cells were predominantly found in the ES-like colonies, where we could also find the high concentration of GFP^+ cells. $CD31^+/GFP^-$ differentiated cells were predominantly located at the bottom of the ES-like colonies (**Figure 5B**). This observation implied that miPS-LLCcm formed the endothelial niche *in vitro*. However, the number of $CD31^+$ cells in the bulk culture was much less

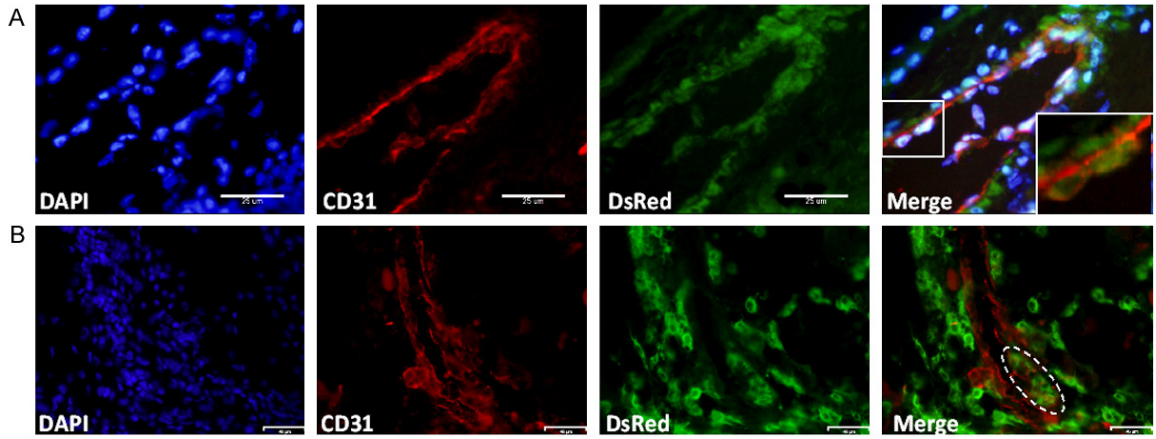

Figure 6. Endothelial differentiation of DsRed-LLCcm *in vivo*. Tumors derived from DsRed-LLCcm cells were stained with CD31 (red) and DsRed (green) antibodies. A: A typical $CD31^+$ endothelial vessel comprised of $DsRed^+$ cells. Scale bar: 25 μm. B: A blood vessel comprised of $CD31^+/DsRed^-$ cells and $CD31^+/DsRed^+$ cells. Scale bar: 58 μm.

than that found in the tubes on Matrigel. Time course of *in vitro* tube development showed that the number of $CD31^+$ cells was gradually increasing (**Figure 5C**). It is highly possible that some of the $CD31^-/GFP^-$ cells acted as endothelial precursor cells, such as $VEGFR2^+$ cells, mature into endothelial cells as $CD31^+/GFP^-$ cells during the culture on Matrigel.

The observation *in vitro* prompted us to investigate whether CSC originated blood vessels *in vivo*. We looked for tubular structures that were $CD31^+/DsRed^+$ double positive in the tumor derived from DsRed-LLCcm cells by immunofluorescence staining. We could find not only these structures (**Figure 6A**), but also mosaic vasculatures, in which blood vessels were mostly formed by $CD31^+/DsRed^-$ cells, which should be derived from host, and $CD31^+/DsRed^+$ cells, which should be derived from DsRed-LLCcm cells (**Figure 6B**). Immunohistochemical analysis of DsRed expression also showed that $DsRed^+$ cells were integrated into blood vessels (**Figure 2D**). These results imply the physical interaction between ECs from host and tumor-derived ECs resulting in the functional connection of tumor-derived blood vessel and host blood vessels.

Vasculogenic mimicry in the tumor of DsRed-LLCcm cells

In many tumors, ECM rich-blood channels, which are lined by tumor cells instead of vascular endothelial cells, so called vasculogenic mimicry (VM), are reported. VM-forming cells have been described as very malignant and poorly differentiated [9]. While we observed blood vessels composed of ECs in the tumor of miPS-LLCcm cells and DsRed-LLCcm cells, we looked into the presence of VM in the tumors. We stained paraffin-embedded sections of the tumors with anti-CD31 antibody and PAS, to investigate ECM rich structures to find VM, which is defined as $CD31^-/PAS^+$ patterns. As the result, we found abundant PAS^+ patterns and tubular blood vessels-like outlines. In this context, approximately 7.6% of all the channels were judged VM while most parts of the structure were not VM as $CD31^+$. Blood cells were frequently observed in the cavities surrounding PAS^+ structures (**Figure 7A**). This indicates that VM was developed in the tumor of DsRed-LLCcm cells. In contrast, tumor derived from LLC cells exhibited little PAS^+ staining (data not shown).

Furthermore, we observed GFP^+ vasculatures (**Figure 7B**, up). Since GFP was used as a reporter of Nanog expression [28, 31], this indicates that the channel was structured by undifferentiated cells. Moreover, these vessels were also PAS^+ (**Figure 7B**, down). Both undifferentiated cells and PAS^+ channels should illustrate VM, and suggests that undifferentiated subpopulation of the CSC model, DsRed-LLCcm cells, participate in the VM formation.

Discussion

The growing evidences indicate that formation of the tumor vascular network is a complex

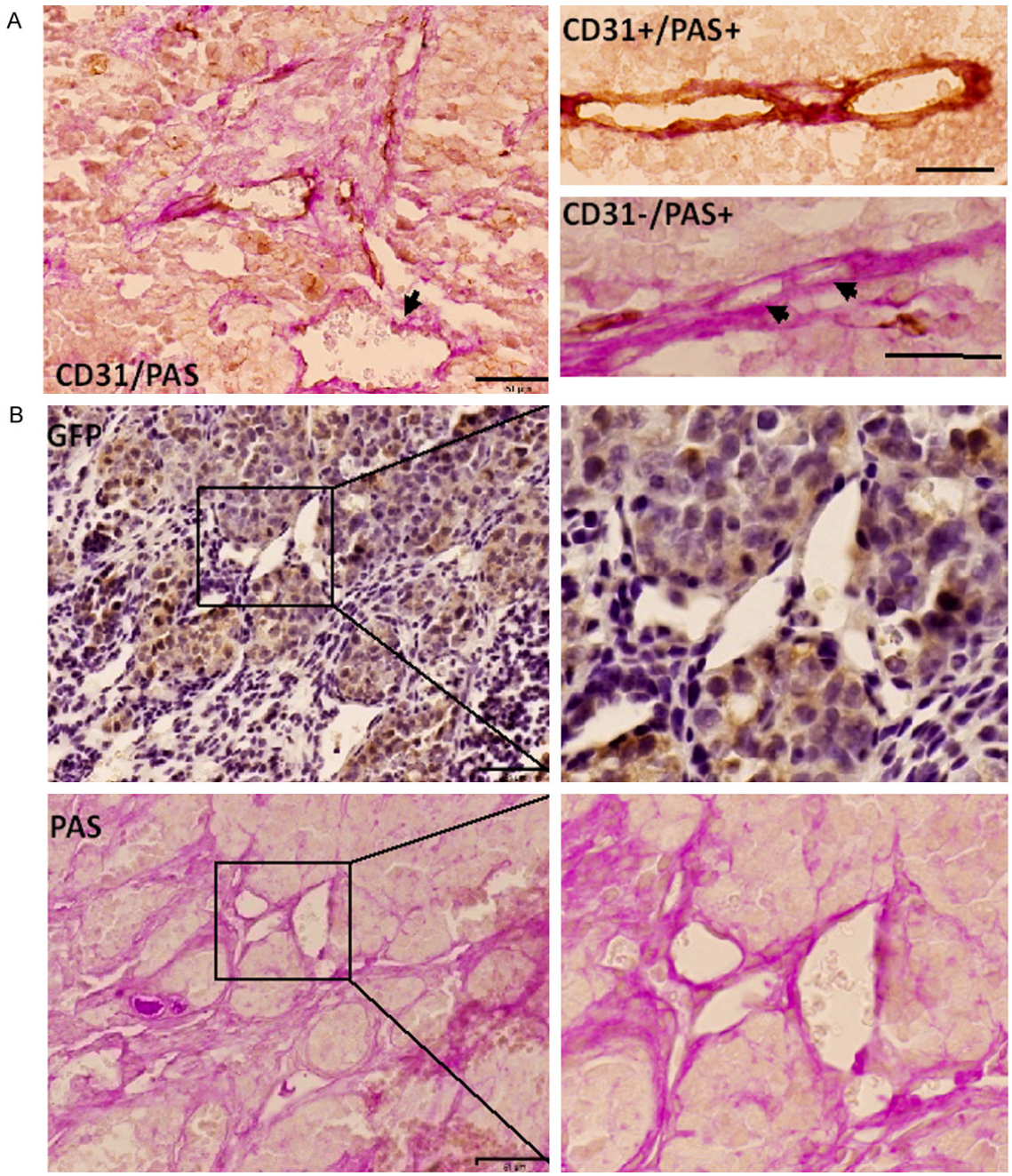

Figure 7. Vasculogenic Mimicry in the DsRed-LLCcm derived tumor. A: Tumor sections were stained with CD31 antibody (brown) and PAS (pink). EC lined vessels ($CD31^+/PAS^-$) and tumor cell lined VMs ($CD31^-/PAS^+$) were observed. Arrows show VM. Scale bar: 50 μm (left), 25 μm (right). B: Immunohistochemistry of GFP (brown) and PAS (Pink) staining in serial sections of tumor derived from DsRed-LLCcm cells. Scale bar: 50 μm.

event in the cancerous niche [3]. Recently two models of tumor vasculogenesis, CSC differentiation into EC and vasculogenic mimicry, emphasize the contribution of CSCs towards tumor vascularization [19, 20]. To analyze the relationship of the two models, we adopted our miPS-LLCcm cell, which is a model of CSC that exhibits self-renewal [29], differentiation, and ability to generate a malignant tumor in nude mice [23, 27]. First of all, we introduced DsRed2 gene into miPS-LLCcm cells, establishing DsRed-LLCcm cells, which constitutively dis-

play red fluorescence. The introduction of DsRed2 gene represents an improvement of miPS-LLCcm model since it allows us to trace miPS-LLCcm throughout the cell differentiation and localization both *in vitro* and *in vivo*. Using miPS-LLCcm and DsRed-LLCcm cells, we found the contribution of CSCs in the various events in tumor vascularization, such as angiogenesis, endothelial differentiation of CSCs, and VM formation.

The angiogenic activity of DsRed-LLCcm, which was confirmed by CAM assay (**Figure 3B**, **3C**) and by the presence of host $CD31^+/DsRed^-$ endothelial vessels derived from the host in the tumor (**Figure 3E**), might be corroborated by the high expression of angiogenic factors in CSCs (**Figure 3D**). It has been shown that Glioma CSCs, defined as the subpopulation expressing the CSC marker CD133, expressed 10 fold more VEGF than the $CD133^-$ subpopulation in both hypoxia and normoxia, inducing the angiogenesis response [32]. This ability of CSC to secrete higher amount of VEGF has been described in breast cancer and malignant gliomas [32-35]. Although it has not been considered directly related with the secretion from CSCs, FGF2 stimulates survival, proliferation, migration and differentiation of EC. Both VEGF and FGF2 have been described to induce angiogenesis in CAM assay [36, 37]. In accordance with these observations, VEGF-A and FGF2 were expressed 6 and 3 folds higher, respectively, in the undifferentiated GFP^+ population of DsRed-LLCcm cells compared to the bulk culture of DsRed-LLCcm cells (**Figure 3D**). This implies that the CSC subpopulation induces the differentiation and proliferation of ECs resulting in the angiogenesis (**Figure 3**).

These angiogenic factors should also contribute to the differentiation of CSCs into ECs. This differentiation was first reported in glioblastoma, in which some EC contained glioma-specific chromosomal aberration indicating that the endothelial cells were derived from tumor cells [20]. Brossa et al. described the differentiation of breast-CSC into endothelial cells required addition of external VEGF or hypoxia [21]. We have also reported that our miPS-LLCcm differentiated into endothelial cells *in vitro* (**Figure 5C**) [27]. Contrasting to breast-CSCs, EC differentiation from miPS-LLCcm cells occurred spontaneously on gelatin-coated dish exhibiting CD31 positive cells, which were readily detectable in the bulk culture (**Figure 5A**, **5B**), resembling an *in vitro* niche. This finding is consistent with the reports describing that ECs secrete factors that will promote survival and self-renewal of CSCs [16, 27, 38].

Even though we observed an increase of $CD31^+$ cells in tube formation we could not determine which was the origin of $CD31^+/GFP^-$ ECs *in vitro*. Studies in glioblastoma have also shown a bipotential $CD31^+/CD133^+$ subpopulation that gave rise to EC via differentiation [19]. These bipotential cells in glioblastoma seems to be equivalents to our $CD31^+/GFP^+$ cells since both cells expressed stem cell marker and endothelial marker. However, as shown in our previous study [27], concentrated GFP^+ miPS-LLCcm cells, which contain $GFP^+/CD31^-$ and $GFP^+/CD31^+$ cells (**Figure 4A**), alone were not able to generate tube-like structures on Matrigel (**Figure 4B**). Similarly, self-renewing spheroids of miPS-LLCcm did not form tube-like structures directly (**Figure 4C**, left). On the other hand, these cells gained the ability to form tube-like structures when the spheroids are allowed to differentiate into adhesive GFP^- cells, which contain $GFP^-/CD31^-$ and $GFP^-/CD31^+$ cells (**Figure 5C**, right), This suggests that the dominant cells responsible to form tubes were GFP^- cells, which were also found to be mostly $CD31^-$ before tube formation and resided outside of ES-like colonies in bulk culture of miPS-LLCcm cells (**Figure 5A**, **5B**). We have previously reported the presence of $VEGFR2^+$ cells, which are considered to be EC precursors, in the GFP^- subpopulation [27]. Taking our previous results together, it is likely that ECs were maturated from $CD31^-/GFP^-$ with VEGFR2 expressing cells as precursors of ECs derived from ES cells were maturated in VEGF dependent manner [39]. Considering the significant expression of VEGF-A and FGF2 from GFP^+ cells (**Figure 3D**), these angiogenic factors should be responsible for the maturation of miPS-LLCcm progenies as ECs in paracrine manner.

The $CD31^+/GFP^+$ bipotential cells in miPS-LLCcm cells might be corresponding to the stem cell/progenitor-like cells, which were considered to differentiate into endothelial cells, present in vascular structures [40]. Recently, stem cell/progenitors excluding Hoechst with

CD31 and other endothelial markers were isolated from mouse normal lung [41]. These cells were found to be involved in the tumor angiogenesis by supplying ECs. Hoechst excluding side population has been recognized as stem cell enriched population in both normal and cancer tissues [42]. Collectively, $CD31^+/GFP^+$ bipotential cells in miPS-LLCcm cells could be one of the origins of CSC-derived ECs *in vivo*. Further investigation is required to identify the exact pathway of CSC differentiation into ECs. Also the CSCs properties, such as the ability to form malignant tumors, of $CD31^+/GFP^+$ bipotential cells should be assessed. The differentiation of DsRed-LLCcm into ECs was confirmed *in vivo* as $CD31^+/DsRed^+$ vessels were found in the tumors although the differentiation process was not clear (**Figure 6A**).

Despite its clinical importance [10], the biological features of the tumor cells that form VM, as well as the cellular and molecular events underlying its formation remain largely unknown. Maniotis et al. suggested that melanoma cells lining VM could have been reverted to an embryonic-like phenotype [14] since they were found to express multiple stemness markers. We observed that 7.6% of all the tumor vasculature in DsRed-LLCcm tumor could be defined as VM, which were ECM-rich vessels lacking of ECs (**Figure 7A**). Furthermore, we detected the presence of GFP^+ undifferentiated cells, reflecting the stemness gene Nanog expression, in PAS^+ channels (**Figure 7B**). These channels were frequently found in the region where most of stromal cells were GFP^+. Although we cannot state that the CSC ability remains in all of the GFP^+ cells including those forming the PAS^+ channel, GFP^+ cells are indeed the ones with the ability of self-renewal (**Figure 1B**) and differentiation (**Figure 4C**).

We have shown that CSCs can differentiate into ECs that are able form vessels as well as contribute to VM formation *in vivo*. Simultaneously, early stages of *in vitro* tube formation showed that these were formed mostly by $CD31^-$ cells (**Figure 5C**). Taking these observations into consideration, we hypothesized that VM could be an intermediate stage of CSC differentiation. Zhang et al. discussed the presence of three kinds of vessels in melanoma, which were VM, mosaic vessels and endothelium patterned vessels. VM was described as the dominant in the early stage of tumor growth, following EC differentiation and proliferation and mosaic vessels would appear as a transitional pattern [16, 43]. Other authors proposed that VM might be CSCs that remain incomplete in differentiation towards the endothelial lineage [19].

In conclusion, miPS-LLCcm and DsRed-LLCcm cells simultaneously exhibited different three types of tumor vasculature in a tumor tissue as angiogenesis, endothelial differentiation from CSCs and formation of VM *in vivo*. The CSC subpopulation of miPS-LLCcm cells donates angiogenic factors not only to attract host endothelial vessels into tumor, but also to promote maturation of endothelial linage of CSC's progenies. miPS-LLCcm would be a powerful model to analyze the interaction of host EC and CSC-derived EC at molecular level, the mechanisms of development of mosaic vessels, and their physiological/pathological relevance. Tumor vasculature is essential for tumor growth; however current therapeutic strategies targeting only angiogenesis are leading to insufficient outcomes. Taking these under consideration, miPS-LLCcm could be an appropriate model to understand entire tumor vascularization and to develop novel drugs and therapeutic strategies.

Acknowledgements

This research was supported by the Grant-in-Aid for Scientific Research (A) No. 25242045 (MS); the Grant-in-Aid for Challenging Exploratory Research No. 26640079 (MS) and the Japan Science and Technology Agency, Matching Planner Program-Tansaku Shiken-Grant.

Disclosure of conflict of interest

None.

Address correspondence to: Akifumi Mizutani and Masaharu Seno, Department of Biotechnology, Graduate School of Natural Science and Technology, Okayama University, 3.1.1 Tsushima-Naka, Kita-ku, Okayama 700-8530, Japan. Tel: +81-86-251-8209; Fax: +81-86-251-8209; E-mail: mizut-a@okayama-u.ac.jp (AM); Tel: +81-86-251-8216; Fax: +81-86-251-8216; E-mail: mseno@okayama-u.ac.jp (MS)

References

[1] Kaur S, Bajwa P. A 'tête-à tête' between cancer stem cells and endothelial progenitor cells in

tumor angiogenesis. Clin Transl Oncol 2014; 16: 115-121.
[2] Hanahan D, Folkman J. Patterns and emerging mechanisms of the angiogenic switch during tumorigenesis. Cell 1996; 86: 353-364.
[3] Butler J, Kobayashi H, Rafii S. Mechanisms of angiogenesis and arteriogenesis. Nat Med 2000; 6: 389-395.
[4] Buttler JM, Kobayashi H, Rafii S. Instructive role of the vascular niche in promoting tumour growth and tissue repair by angiocrine factors. Nat Rev Cancer 2010; 10: 138-146.
[5] Otrocka ZK, Mahfouzb RA, Makarema JA, Shamseddine AI. Understanding the biology of angiogenesis: review of the most important molecular mechanisms. Blood Cells Mol Dis 2007; 39: 212-220.
[6] Cross MJ, Claesson-Welsh L. FGF and VEGF function in angiogenesis: Signalling pathways, biological responses and therapeutic inhibition. Trends Pharmacol Sci 2001; 22: 201-207.
[7] Folkman J. Angiogenesis: an organizing principle for drug discovery? Nat Rev Drug Discov 2007; 6: 273-286.
[8] Bergers G, Hanahan D. Mode of resistance to anti-angiogenic therapy. Nat Rev Cancer 2008; 8: 592-603.
[9] Chen YS, Chen ZP. Vasculogenic mimicry: A novel target for glioma therapy. Chin J Cancer 2014; 33: 74-79.
[10] Maniotis AJ, Folberg R, Hess A, Seftor EA, Gardner LM, Pe'er J, Trent JM, Meltzer PS, Hendrix MJ. Vascular channel formation by human melanoma cells in vivo and in vitro: vasculogenic mimicry. Am J Pathol 1999; 155: 739-752.
[11] Lirdprapamongkol K, Chiablaem K, Sila-Asna M, Surarit R, Bunyaratvej A, Svasti J. Exploring stemness gene expression and vasculogenic mimicry capacity in well- and poorly-differentiated hepatocellular carcinoma cell lines. Biochem Biophys Res Commun 2012; 422: 429-435.
[12] Alameddine RS, Hamieh L, Shamseddine A. From sprouting angiogenesis to erythrocytes generation by cancer stem cells: Evolving concepts in tumor microcirculation. Biomed Res Int 2014; 2014: 986768.
[13] Wagenblast E, Soto M, Gutierrez-Angel S, Hartl CA, Gable AL, Maceli AR, Erard N, Williams AM, Kim SY, Dickopf S, Harrell JC, Smith AD, Perou CM, Wilkinson JE, Hannon GJ, Knott SR. A model of breast cancer heterogeneity reveals vascular mimicry as a driver of metastasis. Nature 2014; 67: 223-230.
[14] Hendrix MJ, Seftor EA, Meltzer PS, Gardner LM, Hess AR, Kirschmann DA, Schatteman GC, Seftor RE. Expression and functional significance of VE-cadherin in aggressive human melanoma cells: role in vasculogenic mimicry. Proc Natl Acad Sci U S A 2001; 98: 8018-8023.
[15] Hess AR, Seftor EA, Gruman LM, Kinch MS, Seftor RE, Hendrix MJ. VE-cadherin regulates EphA2 in aggressive melanoma cells through a novel signaling pathway: Implications for vasculogenic mimicry. Cancer Biol Ther 2006; 5: 228-233.
[16] Yao XH, Ping YF, Bian XW. Contribution of cancer stem cells to tumor vasculogenic mimicry. Protein Cell 2011; 2: 266-272.
[17] Chang YS, di Tomaso E, McDonald DM, Jones R, Jain RK, Munn LL. Mosaic blood vessels in tumors: frequency of cancer cells in contact with flowing blood. Proc Natl Acad Sci U S A 2000; 97: 14608-14613.
[18] Clarke MF, Dick JE, Dirs PB, Eaves CJ, Jamieson CH, Jones DL, Visvader J, Weissman IL, Wahl GM. Cancer stem cells-prespectives on current status and future directions:ACR Workshop on cnacer stem cells. Cancer Res 2006; 66: 9339-9344.
[19] Ricci-Vitiani L, Pallini R, Biffoni M, Todaro M, Invernici G, Cenci T, Maira G, Parati EA, Stassi G, Larocca LM, De Maria R. Tumour vascularization via endothelial differentiation of glioblastoma stem-like cells. Nature 2011; 468: 824-828.
[20] Wang R, Chadalavada K, Wilshire J, Kowalik U, Hovinga KE, Geber A, Fligelman B, Leversha M, Brennan C, Tabar V. Glioblastoma stem-like cells give rise to tumour endothelium. Nature 2010; 468: 829-833.
[21] Brossa A, Grange C, Mancuso L, Annaratone L, Maria Satolli MA, Mazzone M, Camussi G, Bussolati B. Sunitinib but not VEGF blockade inhibits cancer stem cell endothelial differentiation. Oncotarget 2015; 6: 11295-11309.
[22] Yue WY. Does Vasculogenic Mimicry Exist in Astrocytoma? J Histochem Cytochem 2005; 53: 997-1002.
[23] Chen L, Kasai T, Li Y, Sugii Y, Jin G, Okada M, Vaidyanath A, Mizutani A, Satoh A, Kudoh T, Hendrix MJ, Salomon DS, Fu L, Seno M. A model of cancer stem cells derived from mouse induced pluripotent stem cells. PLoS One 2012; 7: e33544.
[24] Murai K, Murakami H, Nagata S. Myeloid-specific transciptional activation by murine myeloid zinc-finger protein 2. Proc Natl Acad Sci U S A 1998; 95: 3461-3466.
[25] Omura T, Sakai H, Murakami H. Acceleration of granulocyte colony-stimulating factor-induced neutrophilic nuclear lobulation by overexpression of Lyn tirosine kinase. Eur J Biochem 2002; 269: 381-389.
[26] Yan T, Mizutani A, Chen L, Sugii Y, Jin G, Okada M, Vaidyanath A, Mizutani A, Satoh A, Kudoh T, Hendrix MJC, Salomon DS, Fu L, Seno M. Char-

acterization of cancer stem-like cells derived from mouse induced pluripotent stem cells transformed by tumor-derived extracellular vesicles. J Cancer 2014; 5: 572-584.
[27] Matsuda S, Yan T, Mizutani A, Sota T, Hiramoto Y, Prieto-Vila M, Chen L, Satoh A, Kudoh T, Kasai T, Murakami H, Fu L, Salomon DS, Seno M. Cancer stem cells maintain a hierarchy of differentiation by creating their niche. Int J Cancer 2014; 135: 27-36.
[28] Okita K, Ichisaka T, Yamanaka S. Generation of germline-competent induced pluripotent stem cells. Nature 2007; 448: 313-317.
[29] Visvader JE, Lindeman GJ. Cancer stem cells in solid tumours: accumulating evidence and unresolved questions. Nat Rev 2008; 8: 755-768.
[30] Blacher S, Devy L, Hlushchuk R, Blacher S, Devy L, Hlushchuk R, Larger E, Lamande N, Burri P, Corvol P, Djonov V, Foidart JM, Noel A. Quantification of angiogenesis in the chicken chorioallantoic membrane (CAM). Image Anal Stereol 2005; 24: 169-180.
[31] Takahashi K, Yamanaka S. Induction of Pluripotent Stem Cells from Mouse Embryonic and Adult Fibroblast Cultures by Defined Factors. Cell 2006; 126: 663-676.
[32] Bao S, Wu Q, Sathornsumetee S, Hao Y, Li Z, Hjelmeland AB, Shi Q, McLendon RE, Bigner DD, Rich JN. Stem cell-like glioma cells promote tumor angiogenesis through vascular endothelial growth factor. Cancer Res 2006; 66: 7843-7848.
[33] Ponti D, Costa A, Zaffaroni N, Pratesi G, Petrangolini G, Coradini D, Pilotti S, Pierotti MA, Daidone MG. Isolation and In vitro Propagation of Tumorigenic Breast Cancer Cells with Stem/Progenitor Cell Properties. Cancer Res 2005; 65: 5506-5511.
[34] Pellegatta S, Poliani PL, Corno D, Menghi F, Ghielmetti F, Suarez-Merino B, Caldera V, Nava S, Ravanini M, Facchetti F, Bruzzone MG, Finocchiaro G. Neurospheres enriched in cancer stem-like cells are highly effective in eliciting a dendritic cell-mediated immune response against malignant gliomas. Cancer Res 2006; 66: 10247-10252.
[35] Lever E, Sheer D. The role of nuclear organization in cancer. J Pathol 2010; 220: 114-125.
[36] Eliceiri BP, Klemke R, Strömblad S, Cheresh DA. Integrin avβ3 requirement for sustained mitogen-activated protein kinase activity during angiogenesis. J Cell Biol 1998; 140: 1255-1263.
[37] Eliceiri BP, Paul R, Schwartzberg PL, Hood JD, Leng J, Cheresh DA. Selective requirement for Src kinases during VEGF-induced angiogenesis and vascular permeability. Mol Cell 1999; 4: 915-924.
[38] Krishnamurthy S, Dong Z, Vodopyanov D, Imai A, Helman JI, Prince ME, Wicha MS, Nör JE. Endothelial cell-initiated signaling promotes the survival and self-renewal of cancer stem cells. Cancer Res 2010; 70: 9969-9978.
[39] Yamashita J, Itoh H, irashima M, Ogawa M, Nishikawa S, Yurugi T, Naito M, Nakao K, Nishikawa S. Flk-1positive cells derived from embryonic stem cells serve as vascular progenitors. Nature 2000; 408: 92-96.
[40] Naito H, Wakabayashi T, Kidoya H, Muramatsu F, Takara K, Eino D, Yamane K, Iba T, Takakura N. Endothelial Side Population Cells Contribute to Tumor Angiogenesis and Antiangiogenic Drug Resistance. Cancer Res 2016; 76: 3200-3210.
[41] Alvarez DF, Huang L, King JA, ElZarrad MK, Yoder MC, Stevens T. Lung microvascular endothelium is enriched with progenitor cells that exhibit vasculogenic capacity. Am J Physiol Lung Cell Mol Physiol 2008; 294: 419-430.
[42] Golebiewska A, Brons NHC, Bjerkvig R, Niclou SP. Critical appraisal of the side population assay in stem cell and cancer stem cell research. Cell Stem Cell 2011; 8: 136-147.
[43] Zhang S, Guo HUA, Zhang D, Zhang W, Zhao X, Ren Z, Sun B. Microcirculation patterns in different stages of melanoma growth. Oncol Rep 2006; 15: 15-20.